CrossMark
click for updates

The relationship between node degree and dissipation rate in networks of diffusively coupled oscillators and its significance for pancreatic beta cells

Marko Gosak,[1,2,3] Andraž Stožer,[1,3] Rene Markovič,[2,4] Jurij Dolenšek,[1] Marko Marhl,[2,3,4] Marjan Slak Rupnik,[1,3,5] and Matjaž Perc[2,6,7]

[1]Institute of Physiology, Faculty of Medicine, University of Maribor, SI-2000 Maribor, Slovenia
[2]Department of Physics, Faculty of Natural Sciences and Mathematics, University of Maribor, SI-2000 Maribor, Slovenia
[3]Center for Open Innovation and Research, Core@UM, University of Maribor, SI-2000 Maribor, Slovenia
[4]Faculty of Education, University of Maribor, SI-2000 Maribor, Slovenia
[5]Center for Physiology and Pharmacology, Medical University of Vienna, A-1090 Vienna, Austria
[6]Department of Physics, Faculty of Sciences, King Abdulaziz University, Jeddah, Saudi Arabia
[7]CAMTP—Center for Applied Mathematics and Theoretical Physics, University of Maribor, SI-2000 Maribor, Slovenia

Self-sustained oscillatory dynamics is a motion along a stable limit cycle in the phase space, and it arises in a wide variety of mechanical, electrical, and biological systems. Typically, oscillations are due to a balance between energy dissipation and generation. Their stability depends on the properties of the attractor, in particular, its dissipative characteristics, which in turn determine the flexibility of a given dynamical system. In a network of oscillators, the coupling additionally contributes to the dissipation, and hence affects the robustness of the oscillatory solution. Here, we therefore investigate how a heterogeneous network structure affects the dissipation rate of individual oscillators. First, we show that in a network of diffusively coupled oscillators, the dissipation is a linearly decreasing function of the node degree, and we demonstrate this numerically by calculating the average divergence of coupled Hopf oscillators. Subsequently, we use recordings of intracellular calcium dynamics in pancreatic beta cells in mouse acute tissue slices and the corresponding functional connectivity networks for an experimental verification of the presented theory. We use methods of nonlinear time series analysis to reconstruct the phase space and calculate the sum of Lyapunov exponents. Our analysis reveals a clear tendency of cells with a higher degree, that is, more interconnected cells, having more negative values of divergence, thus confirming our theoretical predictions. We discuss these findings in the context of energetic aspects of signaling in beta cells and potential risks for pathological changes in the tissue. © 2015 AIP Publishing LLC. [http://dx.doi.org/10.1063/1.4926673]

Self-sustained oscillators are models of naturally oscillating objects, and as such they embrace many concepts in physics, biology, and engineering. Stable dissipative oscillatory dynamics results from the flow of energy or matter through a nonlinear system. If the energy is supplied to the system at a rate at which it is dissipated, ordered, and stable, self-organized oscillations may occur. In general, the stability and robustness of such a dynamical state depend on the dissipative properties of individual oscillators, which in turn determine the important dynamical features, such as synchronization and entraining capability. However, in ensembles of interconnected oscillators, the coupling itself can also significantly affect both robustness and dissipation. Motivated by the fact that many real-life systems are composed of coupled dissipative elements that exhibit complex connectivity patterns, in the present study, we therefore analyze the impact of a heterogeneous network structure on the dissipation rates of oscillators. To this effect, we first examine theoretically and numerically the relationship between node degree and average dissipation of oscillators and show that for networks of diffusively coupled oscillators this relation is linear. Next, we validate this result experimentally by measuring the activity of coupled beta cells within intact mouse pancreatic tissue by means of confocal imaging. On the basis of the measured cellular signals, we extract the intercellular functional connectivity patterns and calculate the average dissipation of individual cells. Our results reveal a clear tendency of cells in the network with a higher node degree having higher dissipation rates, which corroborates and in fact confirms our theoretical predictions. Moreover, our findings point out that the intercellular communication quite noticeably contributes to the energy needs of beta cells, which encompasses important aspects of structural and functional performance of beta cell networks in health and disease.

I. INTRODUCTION

Self-sustained oscillators are models of natural and man-made oscillating objects, and these models are essentially nonlinear. In such systems, the flow of energy through

the system gives rise to ordered self-organized oscillations that are stable against perturbations. Stable oscillatory dynamics results from the balance between energy supply and the rate of its dissipation.[1] Sustained oscillations of the limit cycle type can therefore be viewed as temporal dissipative structures. One of the most striking examples of sustained oscillations are biological rhythms, which manifest themselves widely across temporal and structural scales in living organisms and are crucial to normal function, such that a loss of this capacity leads to dysfunction and disease.[1,2] For instance, rhythmicity is the basic *modus operandi* in the neural, cardiovascular, and hormonal system. At the end of the day, rhythmic changes typically affect many different organ systems within an individual and even in populations of organisms, but their basis is usually oscillations in parameter values of various intra- and intercellular signals. In insulin-producing beta cells in pancreatic islets of Langerhans, oscillatory glycolytic degradation of glucose results in oscillations of intracellular NAD(P)H and ATP, leading to a rhythmic activity of ATP-dependent ion channels.[3,4] According to the consensus model, this results in electrical depolarizations, periodic influx of calcium ions due to increased permeability of voltage-dependent calcium channels, and repolarization due to activation of calcium-dependent potassium channels (and possibly other channels).[5,6] Finally, the calcium-dependent secretion of the hormone insulin occurs in an oscillatory manner.[7,8] The ongoing oscillatory activity is made possible by a constant supply of energy in the form of ATP, which fuels the energy-dependent processes of maintaining ion concentrations, synthesizing the hormone, and recycling the granules at the plasma membrane, to name only a few.[9,10] The aforementioned oscillations are observed across a population of electrically and metabolically coupled beta cells, and this enables that concentrations of insulin in the plasma oscillate, which in turn is crucial for normal glucose sensitivity.[11–14] Loss of normal plasma insulin oscillations is a hallmark of diabetes mellitus, a major public health problem, and a deeper understanding of the mechanistic substrate for the oscillatory behavior is of great practical importance.

Biological oscillators, especially signal transduction pathways, have to be highly flexible in order to be able to precisely adopt their functioning to external signals.[15,16] It has been shown that the flexibility of cellular oscillators depends on the attractive properties of the trajectories in phase space. The strength of attraction is in general defined by the sum of Lyapunov exponents and directly corresponds to the contraction of phase space volume and, hence, to dissipation.[17] Previous studies have pointed out that less dissipative systems can be better synchronized with external periodic inputs,[16] exhibit wider entraining ranges,[17] have better coupling abilities,[18] and are less robust to fluctuations,[19] whereby particular emphasis has also been given to local attractive properties of attractors.[18,20–22] Noteworthy, Wang *et al.*[23] have shown that the robustness of biochemical oscillatory systems with respect to stochastic fluctuations can rigorously be described by means of a probabilistic description of the phase space behavior. In particular, cellular dynamics can be decomposed into the gradient of potential landscape and the divergent free curl flux field, which

provides valuable insights into dissipation costs and stability of oscillatory systems.[23,24] Recently, Menck *et al.*[25] provided a novel theoretical approach for the quantification of the stability of nonlinear systems that is based on the basin stability, which relies on the volume of a state's basin of attraction. Their approach exceeds the traditional linearization-based methods and is therefore suitable for studies of high-dimensional nonlinear systems subjected to non-small perturbations. Furthermore, the relationship between dissipation and flexibility seems to be of special importance for biological systems, since in view of low free energy consumption, dissipation should be minimized.[26] In the view of that, Torrealdea *et al.* derived energy functions of a neuron model in order to study the dissipation and balance of energy by cooperative behavior of neurons, which is of particular importance for the understanding of efficient neuronal information processing and coding.[27,28]

In biological systems, coupling between biological oscillators is a hallmark property reflecting their function. Examples of coupled biological oscillators range from pulsating fireflies at the ecological level[29] to the pacemaker cells of the sinoatrial node in the heart,[30] the network of neurons in circadian pacemakers controlling the sleep-wake cycle,[15,17,31,32] and insulin secreting cells of the pancreas[11,33,34] at the tissue level. Despite their need for the right level of flexibility, biological oscillators must be robust to resist environmental perturbations in order to fulfil their biological function. Circadian clocks must sustain daily oscillations with a given period, yet allowing for entrainment to environmental cues.[35] Relaxation rate upon perturbation (i.e., the rigidity of the synchronized network) is critically determined by coupling between oscillators.[17] An elegant study by Abraham *et al.*[15] showed that coupling makes oscillators more rigid, that is, they relax faster in response to perturbation, whereas decoupling of neurons within suprachiasmatic nucleus facilitated the entraining capability of the tissue, producing weaker oscillators. Most commonly, biological tissues do not share uniform properties; rather they exhibit complexity in the topology of intercellular communications pathways, with noticeable heterogeneity in the number of connections between individual cells. A heterogeneous network structure, however, implies a non-trivial impact on dynamic properties and rigidity of individual oscillators.[36–38] To address these issues more thoroughly, we investigate in the present paper the relationship between topological features of a network and dissipation characteristics of oscillators by means of theoretical, numerical, and experimental approaches.

II. DISSIPATION AND FLEXIBILITY OF COUPLED OSCILLATORS

Let there be N diffusively coupled oscillators. The dynamics of the i-th oscillator can in general be written as the time derivative of the L-dimensional vector of dynamical variables[17,37]

$$\dot{z}_i = F(z_i) + \varepsilon \sum_{j=1}^{N} d_{ij}(z_j - z_i), \tag{1}$$

where ε defines the coupling strength and d_{ij} the binary coupling matrix. The average dissipation of the i-th oscillator can be assessed by the time-averaged divergence[37]

$$\langle \mathrm{div}_i \rangle = \left\langle \sum_{l=1}^{L} \frac{\partial \dot{z}_{i,l}}{\partial z_{i,l}} \right\rangle = \left\langle \sum_{l=1}^{L} \left(\frac{\partial F(z_{i,l})}{\partial z_{i,l}} - \varepsilon k_i \right) \right\rangle, \quad (2)$$

where $\langle \ldots \rangle$ signifies the average over the whole attractor in the phase space and k_i is the degree (number of connections of the i-th node). Divergence directly reflects the level of dissipation in a given dynamical system, which in turn attributes to robustness of the oscillator. Highly robust oscillatory systems are characterised by a more negative divergence of the corresponding attractor, whereas less negative values of the divergence characterise more flexible systems.[39] The first term in the sum in Eq. (2) refers to the so-called intrinsic dissipation, whereas the second term reflects the coupling-induced dissipation.[37] According to Eq. (2), the robustness of an oscillator depends on the coupling and/or its role in the network, whereby these effects are more pronounced in intrinsically flexible oscillatory systems. Importantly, the average dissipation can alternatively also be calculated as the sum of Lyapunov exponents:[40]

$$\langle \mathrm{div}_i \rangle = \sum_{l=1}^{L} \lambda(l)_i, \quad (3)$$

where $\lambda(l)_i$ signifies the l-th Lyaponov exponent of the i-th oscillator and the sum runs over all dimensions of the phase space.

III. COMPUTATIONAL RESULTS

The dynamics of the i-th node in the network will be governed by the paradigmatic Hopf oscillator[17,41,42]

$$\dot{x}_i = \gamma(A - r_i^2)x_i - \omega_i y_i + \varepsilon \Sigma_{j=1}^{N} d_{ij}(x_j - x_i), \quad (4)$$

$$\dot{y}_i = \gamma(A - r_i^2)y_i + \omega_i x_i + \varepsilon \Sigma_{j=1}^{N} d_{ij}(y_j - y_i). \quad (5)$$

In Eqs. (4) and (5), $\dot{x}_i$ and $\dot{y}_i$ are time derivatives of the dynamical variables x_i and y_i, A is the square of the limit cycle radius, r_i is the distance from the origin of phase space to the attractor, ω_i is the angular velocity of the i-th oscillator, ε is the coupling strength, and d_{ij} is the ij-th element of the connectivity matrix. The parameter γ defines the relaxation rate towards the limit cycle and directly reflects the flexibility of an individual Hopf oscillator.[17] In our calculation, we set $\varepsilon = 0.4$, $\gamma = 2.0$, and $A = 1.0$. We additionally introduce some variability of oscillators by randomly distributing the angular frequencies, which are assumed to follow a normal distribution with a mean value $\omega_0 = 2\pi$ and a relative standard deviation $0.05\omega_0$.

For the modelling of the interaction topology, we make use of the modulated Barabási-Albert model in Euclidean space.[43] In addition to the original preferential attachment mechanism,[44] the model encompasses weighting of probabilities for connections with physical length. The network growth starts with n_0 points randomly distributed on a unit square with $n = 2 < n_0$ connections among them. In every time step, new one node is introduced with randomly chosen coordinates. The new node establishes m connections with its predecessors i with an attachment probability

$$\Pi_i \sim k_i I_i^{\alpha}, \quad (6)$$

where k_i and I_i are the degree and the distance to the i-th predecessor, respectively. Parameter α in Eq. (6) is the modulation factor that restricts the length of connections and thereby impacts the topology. In order to study the oscillatory dynamics on different network structures, we use in our calculations three different values of α. For $\alpha = 0$, the attachment solely depends on node degrees, which results in the generation of a scale-free network with dominating long-range connections (Fig. 1(a)). To additionally include the impact of spatial embedding, we use in the second case $\alpha = -3.0$, so that an intermediate heterogeneous network with long- and short-range interactions is constructed (Fig. 1(b)). Finally, for $\alpha = -10$, the Euclidean distance is the key agent that determinates the preferential attachment procedure. Accordingly, a rather homogeneous network is generated with mostly adjacent nodes being connected.

Let us now populate the three generated networks presented in Figs. 1(a)–1(c) with Hopf oscillators, whereby the network structure determinates the coupling matrix d_{ij}. To quantify the dissipation rate of a particular oscillator in the network, we derived its Jacobian matrix $\boldsymbol{J}_i$

$$\boldsymbol{J}_i = \begin{pmatrix} \gamma(A - r_i^2) - 2\gamma x_i^2 - \varepsilon k_i & -\omega_i - 2\gamma x_i y_i \\ -\omega_i - 2\gamma x_i y_i & \gamma(A - r_i^2) - 2\gamma y_i^2 - \varepsilon k_i \end{pmatrix}. \quad (7)$$

The divergence of the phase space equals the trace of the Jacobian matrix $Tr(\boldsymbol{J}_i) = 2\gamma(A - 2r_i^2) - 2\varepsilon k_i$. Accordingly, the average divergence for the Hopf oscillator can be expressed as

$$\langle \mathrm{div}_i \rangle = \langle 2\gamma(A - 2r_i^2) - 2\varepsilon k_i \rangle. \quad (8)$$

For the numerical calculation of the average divergence, we evolve the system and calculate at each integration step the current divergence value. The average is then based on the calculations over 100 periods. It should be noted that similar concepts of stability analysis have already been successfully applied, for example, to study the synchronization behavior of Hopf oscillators in star-like networks[42] and the occurrence of oscillation death in networks with repulsive coupling.[45]

Despite the intrinsic symmetry of the attractor, the divergence may vary with time due to perturbations of the limit cycle provoked by the influence of neighboring oscillators. Results showing the relationship between average divergence and the corresponding node degree for all three networks are shown in Fig. 1. In particular, in Figs. 1(a)–1(c), the colors of nodes signify the average divergence of individual oscillators $\langle \mathrm{div}_i \rangle$. Evidently, oscillators
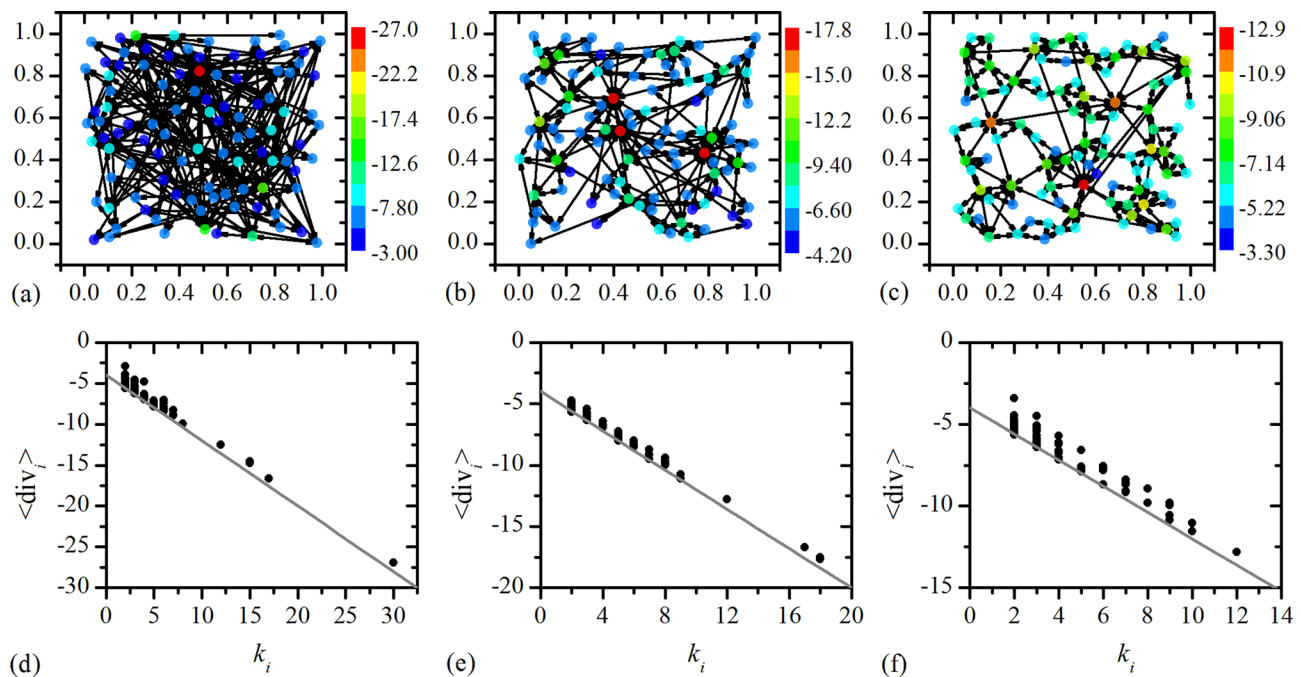
FIG. 1. Characteristic network structures generated with the modulated preferential attachment mechanism for $\alpha = 0$ (a), $\alpha = -3$ (b), and $\alpha = -10$ (c). The number of nodes is $N = 100$. Colors of the nodes signify the average divergence of individual oscillators div$_i$, as indicated by the color bars. In panels (d)–(f), the average divergence as a function of the node degree for the corresponding network structures is shown. The black dots denote the numerically calculated values, whereas the grey lines represent the theoretical prediction given in Eq. (9): $\langle \text{div}_i \rangle = -0.8k_i - 4$.

governing the dynamics of nodes with higher degrees have a more negative average divergence, that is, higher dissipation rates. To quantify this visual assessment, we present in Figs. 1(d)–1(f) individual divergences $\langle \text{div}_i \rangle$ as a function of the corresponding node degree k_i. An obvious linearly decreasing trend can be observed for all three networks.

Next, we compare the numerical results with theoretical predictions. By assuming that the oscillators are in a periodic steady-state, we set $r_i = A = 1$. Accordingly, the relation between average divergence and node degree (see Eq. (8)) can be expressed as

$$\langle \text{div}_i \rangle = -2\gamma - 2\varepsilon k_i. \qquad (9)$$

The first term in Eq. (9) refers to the oscillator's intrinsic divergence, whereas the second term signifies the impact of coupling.[37] The resulting linear relationship between dissipation rates of the i-th oscillator and its node degree is shown in Figs. 1(d)–1(f) with a grey line, whereby the parameter values used in our numerical calculation have been considered ($\gamma = 2.0$ and $\varepsilon = 0.4$). A good agreement between theoretical and numerical results can be observed, except that the numerically calculated values a bit higher. Namely, diffusive coupling provokes a slight decrease in amplitude,[17,46] which implies a less negative divergence. Moreover, deviations from the linear trend are detected, which is predominately ascribed to interactions between heterogeneous oscillators in a heterogeneous network, which results in perturbations of limit cycles. In our calculations, we use $N = 100$ oscillators. It should be noted that the results are more or less independent on choice of the systems size, except for very large ensembles of oscillators, where the connectivities of the

most connected oscillators could result in a collapse of their phase spaces, that is, in oscillation death.[47]

IV. EXPERIMENTAL RESULTS

Recent advances in the field of modern complex network theory have provided novel methodological concepts that enable the investigation of interactions within diverse complex systems, such as stock markets,[48] climate models,[49,50] and various scales of living organisms.[51–54] Recently, these techniques have also been successfully applied for studying collective dynamics of cell populations within intact tissues.[34,55,56] In this paper, we make use of this methodology in order to study the interplay between the intercellular network structure between pancreatic beta cells and the corresponding characteristics of intracellular Ca^{2+} signals. For this purpose, we employed functional multicellular calcium imaging (fMCI) of fluorescently labelled acute mouse pancreas tissue slices to record calcium signals, as described previously.[33,34] The fMCI enables the assessment of Ca^{2+} dynamics in a large number of cells simultaneously, with a high spatiotemporal resolution and over extended periods of time.

The recorded time series were subject to Huang-Hilbert type empirical model decomposition (EEMD)[57] in order to retrieve baseline trends and artefacts, such as bleaching of the fluorescent dye and noise, as described previously.[56] A typical raw signal and the corresponding filtered signal of the temporal evolution of $[Ca^{2+}]_i$ in a beta cell after stimulation with glucose is shown in Fig. 2(a). Both time series were rescaled to the unit interval. It can be observed that the beta cells stimulated with glucose exhibit a well-pronounced oscillatory activity of $[Ca^{2+}]_i$.
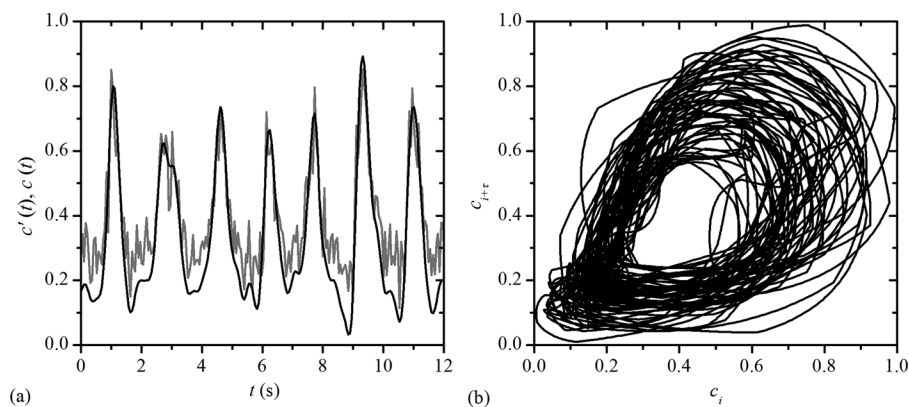
FIG. 2. (a) An excerpt of the fMCI time series capturing the beta cell $[Ca^{2+}]_i$ dynamics provoked by 12 mM glucose in a typical cell. The grey line shows the original recording $c'(t)$ and the black line shows the corresponding EEMD processed signal $c(t)$. (b) Two-dimensional projections of the reconstructed phase space for $\tau = 0.21$ s and $m = 5$.

To quantify the dynamics of the purified time traces, we use the methodology of nonlinear time series analysis.[58] We reconstruct the phase space of $c_i'(t)$ in accordance with the embedding theorem.[59,60] This theorem states that for a large enough embedding dimension m, the delay vectors $z_i(t)$ produce a phase space, which has equal properties as the phase space, formed by the actual variables of the system. The delay vector has the form

$$z_i(t) = [c_i'(t), c_i'(t+\tau), c_i'(t+2\tau), ..., c_i'(t+(m-1)\tau)].$$
(10)

Elements in the delay vector represent the decomposed time traces at discrete times $t, t+\tau, t+2\tau, ..., t+(m-1)\tau$, here τ is the embedding delay. To make a proper reconstruction, we have to determine the parameters m and τ. The estimation of the embedding delay is based on the mutual information method. With it, we can measure the amount of information we have about the state $c_i'(t+\tau)$ presuming we know $c_i'(t)$. Following Fraser and Swinney,[61] the first minimum of mutual information is used as the optimal embedding delay. The estimation of the embedding dimension m is based on the false nearest neighbor method,[62] which relies on the assumption that the system folds and unfolds with no sudden irregularities. Neighboring points in reconstructed phase space will thus stay close during forward integration, and true neighbors cannot grow further apart than δC_{TH}, where C_{TH} is a given constant and δ is the initial separation between two neighboring points. If, on the other hand, a neighbor does not fulfil this criterion, then it is marked as a false nearest neighbor. The minimization of false nearest neighbors is realized with a sufficiently large m. The two-dimensional projections of the reconstructed phase space for a given decomposed time series are shown in Fig. 2(b). To study more thoroughly the dynamics of the given time traces, we estimate the Lyapunov exponents $\lambda(l)_i$, where the index i corresponds to the i-th decomposed time series and l to the l-th Lyapunov exponent. Similarly to eigenvalues, the Lyapunov exponents are an invariant feature of a given system and quantify the average local degrees of the attractor's expansion and contraction.[63] Knowing all of the Lyapunov exponents of a given time trace thus enables us to compute its divergence by summarizing all m Lyapunov exponents. For the calculation of the Lyapunov spectrum, we made use of the radial basis functions for the approximation of the

flow in the phase space,[64,65] thereby receiving an estimation of the average divergence of individual cells.

Next, we construct functional networks on the basis of pairwise correlations between $[Ca^{2+}]_i$ signals of individual cells.[34] Briefly, the correlation matrix R with the ij-th element being the correlation coefficient R_{ij} between the i-th and j-th trace was calculated from the decomposed temporal traces. Functional connections among beta cells are established among those cell pairs, whose correlation coefficient exceeds a threshold value R_{th}. The value of R_{th} determined in such a way, that at least 50% of the variation in system, can be explained with a linear relationship among a cell pair (we use $R_{th} = 0.72$).

To quantify the degree of dissipation of individual beta cells and link it with network characteristics, we color-coded individual nodes in the functional network shown in Fig. 3(a). It can be observed that highly connected nodes exhibit higher dissipation rates, which is well in agreement with our theoretical predictions (see Eq. (2)) and numerical results (Fig. 1). For a more precise description of this observation, we present in Fig. 3(b) the average dissipation of individual cells as a function of their degrees. To ensure a better statistical accuracy, we performed this calculation for four different functional networks being composed of altogether 118 cells. Since absolute values of average divergence varied between different slices, we normalized $\langle div_i \rangle$ between -1 and 0. Analogously, we normalized the degree of each cell to the maximal node degree k_{max} in the respective islet. In this manner, we obliterated the effect of somewhat different network sizes and maximal degrees and were thus able to compare trends in all networks. Nevertheless, the results presented in Fig. 3(b) clearly demonstrate that in all four functional networks, cells with higher degrees, that is, with more functional connections, exhibit higher levels of dissipation ($R^2 = 0.56$ for all data combined). The relationship is not as close as for the theoretical and numerical predictions. There are at least two very important possible reasons for this. First, the experimentally recorded traces are inherently noisy, with the signal-to-noise ratio being different for different islets and individual cells within a single islet. This necessarily leads to inaccuracies in determining the dissipation rates and probably accounts for a part of dispersion. On the other hand, in many aspects of their functioning, beta cells are intrinsically very heterogeneous, and this heterogeneity is only partially reduced following
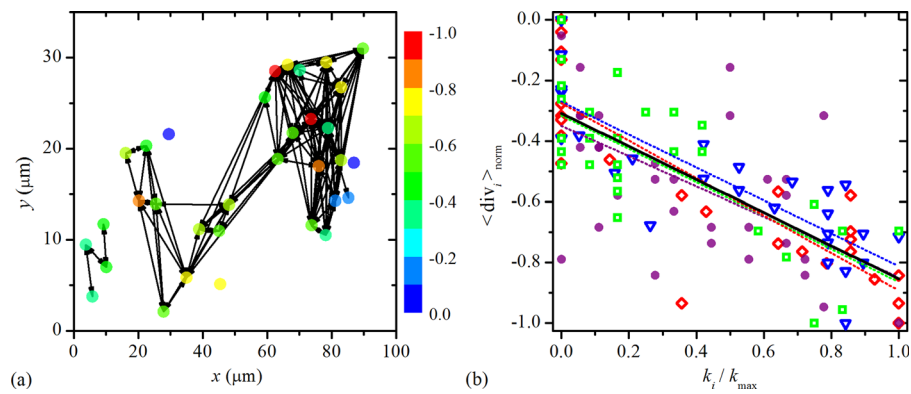
FIG. 3. (a) Functional network architecture of beta cells in a single islet of Langerhans. Each circle represents the physical position of a cell inside the islet. Cells whose correlation exceeds $R_{th} = 0.72$ are considered to be connected. Colors of circles denote the average divergence calculated as the sum of Lyapunov exponents scaled to the unit interval $\langle \mathrm{div}_i \rangle_{norm}$, as indicated by the color bar. (b) The average normalized divergence $\langle \mathrm{div}_i \rangle_{norm}$ as a function of normalized node degree k_i/k_{max} for four different functional networks, as indicated by different symbols and colors. The dotted lines with the corresponding color denote the linearly decreasing trend for individual networks and the black solid line signifies the mutual trend for all data ($R^2 = 0.29$, 0.53, 0.68, and 0.73 for the individual networks, $R^2 = 0.56$ for all data combined).

coupling.[56,66–68] Thus, it is reasonable to assume that beta cells with the same number of connections will show some level of heterogeneity in their dissipation rates. To sum up, intercellular coupling leads to a lower average divergence, as indicated in our theoretical predictions.

V. DISCUSSION

Coupling is known to affect the limit cycle behavior and dynamical characteristics of individual oscillatory elements. It has been shown that coupling makes an oscillator more rigid[15,17,36,37] and can even lead to a collapse of the phase space, that is, oscillation death.[47] In the present study, we systematically analyzed the distribution of dissipation rates of individual oscillators forming a heterogeneous network structure. Our theoretical and experimental results showed that highly connected oscillators in the networks have the highest rates of dissipation. The theoretical results of our mathematical model indicate that dissipation depends on the number of neighbors and the conductance of the coupling channels, that is, coupling strength. In particular, stronger coupling contributes to a higher dissipation rate of an oscillator. Furthermore, from practical point of view, the observed well-pronounced relationship between node degree and the dissipation rates suggests that the divergence of the oscillators can provide additional insights for the reconstruction of the topology of the underlying network of oscillatory elements.

Our findings are in agreement with previous studies of Abraham *et al.*[15] who showed that coupling makes an oscillator more rigid, and on this basis they succeeded to explain the regulation of the entrainment range of circadian clocks by modifying the strength of coupling in the suprachiasmatic nucleus in the hypothalamus. From a physiological point of view, stronger coupling means larger ionic currents and a greater degree of energy consumption, which is also consistent with a greater dissipation. Thus, regulation by coupling might represent an important regulatory mechanism in biological systems. It should be noted, however, that this kind of regulation is only possible if the individual oscillators are inherently flexible in the first place. For an efficient

regulation by coupling, the intrinsic dissipation needs to be comparable with the increase in dissipation caused by coupling. If, namely, the intrinsic dissipation of an oscillator is very large from the outset, that is, much larger than the dissipation shift caused by coupling, then the coupling-induced increase in the dissipation will have a very small effect on the dissipation of the oscillator, and no effective regulation by coupling is possible. On the other hand, if the oscillators are flexible with relatively small intrinsic dissipation rates, then the dissipation will be highly influenced by coupling; and the variety in dissipation rates of the coupled oscillators will be ensured, and hence an effective regulation by coupling is possible.

Our experimental results show that the divergence of cellular oscillators, that is, beta cells in slices of mouse pancreatic tissues, considerably depends on coupling (Fig. 3(b)). The coupling has obviously a strong enough effect to determine the flexibility of the cellular oscillators, which implies that beta cells are inherently flexible and that their intrinsic dissipation must be low enough, as to permit changes upon coupling. This in turn also indicates that the energy required for the intercellular communication is not negligible in comparison with the energetic needs of intracellular signalization. This flexibility of beta cells might play an important role in regulation of insulin secretion in islets of Langerhans. However, this kind of regulation in general is not trivial, and the question arises how flexible cellular oscillators are able to efficiently communicate in cellular networks and provide correlated collective responses in tissues, such as insulin secretion in islets of Langerhans, for example. In our previous studies,[36,37] we showed that flexible oscillators characterized by low dissipation rates synchronize best in the so-called broad-scale small-world networks—a topological feature that is very common in a variety of biological systems.[32,52,69] Most importantly, we have also found these topological characteristics for the networks of pancreatic beta cells.[34] Taken together, we might conclude that there is strong evidence that beta cells in islets of Langerhans operate as flexible cellular oscillators being interconnected in small-world network topologies, which provides an efficient and

robust system for coordinated collective activity. Moreover, since the flexible oscillators have lower dissipation rates and hence lower energy consumption and since in broad-scale small world-networks, there are a large number of cells with few connections and a smaller number of cells with many connections, this type of organization might provide the optimal efficiency not only by communication capabilities but also in terms of energy consumption.

The most interconnected cells, the so-called hubs, have the largest dissipation rates and hence the higher rates of energy consumption. This high energy-turnover of the hubs might have important physiological consequences. The hubs in the functional network overlap with the most connected cells in the anatomic network of the tissue,[70] and these highly connected cells might be strongly affected in pathophysiological conditions. It is known, for instance, that in the compensated phase of type 2 diabetes mellitus, the activity of beta cells increases to supply for the increased demand of insulin.[71] It is thus reasonable to speculate that in type 2 diabetes mellitus, the energetic demand in beta cells increases and that this might mostly affect the hubs, which operate at a higher basal level of energy consumption. Consequently, during the progress of the disease, the network of beta cells would gradually change and this would affect its function. We might expect that the disappearance of hubs would manifest itself as a reduced complexity of the network topology of beta cells, changing gradually from a heterogeneous and efficient small-world topology to a more regular one. However, the decrease in beta cell mass during this progress would be relatively low, since the number of hubs in a network is lower than the number of less well-connected cells. Indeed, it has been shown that in T2D patients with less than 5 years of disease duration, the number of beta cells is reduced by 24%, and it has been suggested that this decrease is unlikely to be able to cause overt diabetes in the absence of concomitant beta cell dysfunction.[72] Although our line of reasoning is only a hypothesis that needs a rigorous experimental validation, it opens a new perspective in understanding of diabetes and it might lead to important clinical applications in the future.

ACKNOWLEDGMENTS

[1] A. Goldbeter, "Biological rhythms as temporal dissipative structures," Adv. Chem. Phys. **135**, 253–295 (2007).

[2] C. S. Nunemaker and L. S. Satin, "Episodic hormone secretion: A comparison of the basis of pulsatile secretion of insulin and GnRH," Endocrine **47**, 49–63 (2014).

[3] R. Bertram, L. S. Satin, M. G. Pedersen, D. S. Luciani, and A. Sherman, "Interaction of glycolysis and mitochondrial respiration in metabolic oscillations of pancreatic islets," Biophys. J. **92**, 1544–1555 (2007).

[4] M. G. Pedersen, E. Mosekilde, K. S. Polonsky, and D. S. Luciani, "Complex patterns of metabolic and Ca2+ entrainment in pancreatic islets by oscillatory glucose," Biophys. J. **105**, 29–39 (2013).

[5] P. Gilon and J.-C. Henquin, "Influence of membrane potential changes on cytoplasmic Ca2+ concentration in an electrically excitable cell, the insulin-secreting pancreatic B-cell," J. Biol. Chem. **267**, 20713–20720 (1992).

[6] J. Marquard *et al.*, "Characterization of pancreatic NMDA receptors as possible drug targets for diabetes treatment," Nat. Med. **21**, 363–372 (2015).

[7] P. Bergsten, E. Grapengiesser, E. Gylfe, A. Tengholm, and B. Hellman, "Synchronous oscillations of cytoplasmic Ca2+ and insulin release in glucose-stimulated pancreatic islets," J. Biol. Chem. **269**, 8749–8753 (1994).

[8] P. Gilon, R. M. Shepherd, and J.-C. Henquin, "Oscillations of secretion driven by oscillations of cytoplasmic Ca2+ as evidences in single pancreatic islets," J. Biol. Chem. **268**, 22265–22268 (1993).

[9] J. Suckale and M. Solimena, "The insulin secretory granule as a signaling hub," Trends Endocrinol. Metab. **21**, 599–609 (2010).

[10] C. B. Wollheim and G. W. Sharp, "Regulation of insulin release by calcium," Physiol. Rev. **61**, 914–973 (1981).

[11] J. Dolenšek, A. Stožer, M. S. Klemen, E. W. Miller, and M. S. Rupnik, "The relationship between membrane potential and calcium dynamics in glucose-stimulated beta cell syncytium in acute mouse pancreas tissue slices," PLoS One **8**, e82374 (2013).

[12] W. S. Head, M. L. Orseth, C. S. Nunemaker, L. S. Satin, D. W. Piston, and R. K. Benninger, "Connexin-36 gap junctions regulate in vivo first- and second-phase insulin secretion dynamics and glucose tolerance in the conscious mouse," Diabetes **61**, 1700–1707 (2012).

[13] G. A. Rutter, T. J. Pullen, D. J. Hodson, and A. Martinez-Sanchez, "Pancreatic *β*-cell identity, glucose sensing and the control of insulin secretion," Biochem. J. **466**, 203–218 (2015).

[14] L. S. Satin, P. C. Butler, J. Ha, and A. S. Sherman, "Pulsatile insulin secretion, impaired glucose tolerance and type 2 diabetes," Mol. Aspects Med. **42**, 61–77 (2015).

[15] U. Abraham, A. E. Granada, P. O. Westermark, M. Heine, A. Kramer, and H. Herzel, "Coupling governs entrainment range of circadian clocks," Mol. Syst. Biol. **6**, 438–13 (2010).

[16] M. Marhl and S. Schuster, "Under what conditions signal transduction pathways are highly flexible in response to external forcing? A case study on calcium oscillations," J. Theor. Biol. **224**, 491–500 (2003).

[17] G. Bordyugov, A. Granada, and H. Herzel, "How coupling determines the entrainment of circadian clocks," Eur. Phys. J. B **82**, 227–234 (2011).

[18] M. Perc and M. Marhl, "Local dissipation and coupling properties of cellular oscillators: A case study on calcium oscillations," Bioelectrochemistry **62**, 1–10 (2004).

[19] U. Kummer, B. Krajnc, J. Pahle, A. K. Green, C. J. Dixon, and M. Marhl, "Transition from stochastic to deterministic behavior in calcium oscillations," Biophys. J. **89**, 1603–1611 (2005).

[20] M. Marhl and M. Perc, "Determining the flexibility of regular and chaotic attractors," Chaos, Solitons Fractals **28**, 822–833 (2006).

[21] M. Perc and M. Marhl, "Synchronization of regular and chaotic oscillations: The role of local divergence and the slow passage effect—A case study on calcium oscillations," Int. J. Bifurcation Chaos **14**, 2735–2751 (2004).

[22] M. Perc and M. Marhl, "Frequency dependent stochastic resonance in a model for intracellular Ca2+ oscillations can be explained by local divergence," Physica A **332**, 123–140 (2004).

[23] J. Wang, L. Xu, and E. Wang, "Potential landscape and flux framework of nonequilibrium networks: Robustness, dissipation, and coherence of biochemical oscillations," Proc. Natl. Acad. Sci. U.S.A. **105**, 12271–12276 (2008).

[24] J. Wang, C. Li, and E. Wang, "Potential and flux landscapes quantify the stability and robustness of budding yeast cell cycle network," Proc. Natl. Acad. Sci. U.S.A. **107**, 8195–8200 (2010).

[25] P. J. Menck, J. Heitzig, N. Marwan, and J. Kurths, "How basin stability complements the linear-stability paradigm," Nat. Phys. **9**, 89–92 (2013).

[26] J. W. Stucki, M. Compiani, and S. R. Caplan, "Efficiency of energy conversion in model biological pumps. Optimization by linear nonequilibrium thermodynamic relations," Biophys. Chem. **18**, 101–109 (1983).

[27]A. Moujahid, A. d'Anjou, F. J. Torrealdea, and F. Torrealdea, "Energy and information in Hodgkin-Huxley neurons," Phys. Rev. E **83**, 031912 (2011).

[28]F. J. Torrealdea, A. d'Anjou, M. Grana, and C. Sarasola, "Energy aspects of the synchronization of model neurons," Phys. Rev. E **74**, 011905 (2006).

[29]J. Buck, "Synchronous rhythmic flashing of fireflies. II," Q. Rev. Biol. **63**, 265–289 (1988).

[30]R. Wilders and H. J. Jongsma, "Beating irregularity of single pacemaker cells isolated from the rabbit sinoatrial node," Biophys. J. **65**, 2601–2613 (1993).

[31]S. J. Aton and E. D. Herzog, "Come together, right…now: Synchronization of rhythms in a mammalian circadian clock," Neuron **48**, 531–534 (2005).

[32]C. Bodenstein, M. Gosak, S. Schuster, M. Marhl, and M. Perc, "Modeling the seasonal adaptation of circadian clocks by changes in the network structure of the suprachiasmatic nucleus," PLoS Comput. Biol. **8**, e1002697 (2012).

[33]A. Stozer, J. Dolensek, and M. S. Rupnik, "Glucose-stimulated calcium dynamics in islets of Langerhans in acute mouse pancreas tissue slices," PLoS One **8**, e54638 (2013).

[34]A. Stožer, M. Gosak, J. Dolenšek, M. Perc, M. Marhl, M. S. Rupnik, and D. Korošak, "Functional connectivity in islets of Langerhans from mouse pancreas tissue slices," PLoS Comput. Biol. **9**, e1002923 (2013).

[35]J. B. Hogenesch and E. D. Herzog, "Intracellular and intercellular processes determine robustness of the circadian clock," FEBS Lett. **585**, 1427–1434 (2011).

[36]R. Marković, M. Gosak, and M. Marhl, "How optimal synchronization of oscillators depends on the network structure and the individual dynamical properties of the oscillators," J. Phys. Conf. Ser. **410**, 012044 (2013).

[37]R. Marković, M. Gosak, and M. Marhl, "Broad-scale small-world network topology induces optimal synchronization of flexible oscillators," Chaos, Solitons Fractals **69**, 14–21 (2014).

[38]C. Zhou and J. Kurths, "Hierarchical synchronization in complex networks with heterogeneous degrees," Chaos **16**, 015104 (2006).

[39]M. Perc and M. Marhl, "Sensitivity and flexibility of regular and chaotic calcium oscillations," Biophys. Chem. **104**, 509–522 (2003).

[40]A. Wolf, J. B. Swift, H. L. Swinney, and J. A. Vastano, "Determining Lyapunov exponents from a time series," Physica D **16**, 285–317 (1985).

[41]V. M. Eguíluz, M. Ospeck, Y. Choe, A. J. Hudspeth, and M. O. Magnasco, "Essential nonlinearities in hearing," Phys. Rev. Lett. **84**, 5232–5234 (2000).

[42]M. Frasca, A. Bergner, J. Kurths, and L. Fortuna, "Bifurcations in a star-like network of Stuart-Landau oscillators," Int. J. Bifurcation Chaos **22**, 1250173 (2012).

[43]S. S. Manna and P. Sen, "Modulated scale-free network in Euclidean space," Phys. Rev. E **66**, 066114 (2002).

[44]A. L. Barabasi and R. Albert, "Emergence of scaling in random networks," Science **286**, 509–512 (1999).

[45]C. R. Hens, O. I. Olusola, P. Pal, and S. K. Dana, "Oscillation death in diffusively coupled oscillators by local repulsive link," Phys. Rev. E **88**, 034902 (2013).

[46]Z. Hou and H. Xi, "Oscillator death on small-world networks," Phys. Rev. E **68**, 055103–055104 (2003).

[47]A. Koseska, E. Volkov, and J. Kurths, "Oscillation quenching mechanisms: Amplitude vs. oscillation death," Phys. Rep. **531**, 173–199 (2013).

[48]G. Bonanno, G. Caldarelli, F. Lillo, and R. N. Mantegna, "Topology of correlation-based minimal spanning trees in real and model markets," Phys. Rev. E **68**, 046130 (2003).

[49]J. F. Donges, Y. Zou, N. Marwan, and J. Kurths, "Complex networks in climate dynamics," Eur. Phys. J.: Spec. Top. **174**, 157–179 (2009).

[50]J. H. Feldhoff, S. Lange, J. Volkholz, J. F. Donges, J. Kurths, and F. W. Gerstengarbe, "Complex networks for climate model evaluation with application to statistical versus dynamical modeling of South American climate," Clim. Dynam. **44**, 1567–1581 (2015).

[51]A. L. Barabasi and Z. N. Oltvai, "Network biology: Understanding the cell's functional organization," Nat. Rev. Genet. **5**, 101–113 (2004).

[52]E. Bullmore and O. Sporns, "Complex brain networks: Graph theoretical analysis of structural and functional systems," Nat. Rev. Neurosci. **10**, 186–198 (2009).

[53]D. G. Green and S. Sadedin, "Interactions matter—Complexity in landscapes and ecosystems," Ecol. Complex. **2**, 117–130 (2005).

[54]G. Weng, U. S. Bhalla, and R. Iyengar, "Complexity in biological signaling systems," Science **284**, 92–96 (1999).

[55]D. J. Hodson, R. K. Mitchell, E. A. Bellomo, G. Sun, L. Vinet, P. Meda, D. Li, W.-H. Li, M. Bugliani, P. Marchetti, D. Bosco, L. Piemonti, P. Johnson, S. J. Hughes, and G. A. Rutter, "Lipotoxicity disrupts incretin-regulated human beta cell connectivity," J. Clin. Invest. **123**, 4182–4194 (2013).

[56]R. Markovic, A. Stožer, M. Gosak, J. Dolenšek, M. Marhl, and M. S. Rupnik, "Progressive glucose stimulation of islet beta cells reveals a transition from segregated to integrated modular functional connectivity patterns," Sci. Rep. **5**, 7845 (2015).

[57]N. E. Huang, Z. Shen, S. R. Long, M. C. Wu, H. H. Shih, Q. Zheng, N.-C. Yen, C. C. Tung, and H. H. Liu, "The empirical mode decomposition and the Hilbert spectrum for nonlinear and non-stationary time series analysis," Proc. R. Soc. London, Ser. A **454**, 903–995 (1998).

[58]H. Kantz and T. Schreiber, *Nonlinear Time Series Analysis* (Cambridge University Press, Cambridge, 2004).

[59]T. Sauer, J. Yorke, and M. Casdagli, "Embedology," J. Stat. Phys. **65**, 579–616 (1991).

[60]F. Takens, *Detecting Strange Attractors in Turbulence* (Springer, Berlin, 1981), pp. 366–381.

[61]A. M. Fraser and H. L. Swinney, "Independent coordinates for strange attractors from mutual information," Phys. Rev. A **33**, 1134 (1986).

[62]M. B. Kennel, R. Brown, and H. D. Abarbanel, "Determining embedding dimension for phase-space reconstruction using a geometrical construction," Phys. Rev. A **45**, 3403 (1992).

[63]D. Kugiumtzis, B. Lillekjendlie, and N. Christophersen, "Chaotic time series. Part I. Estimation of some invariant properties in state space," Model. Identif. Control **15**, 205–228 (1994).

[64]B. Krese, M. Perc, and E. Govekar, "The dynamics of laser droplet generation," Chaos **20**, 013129 (2010).

[65]U. Parlitz, "Identification of true and spurious Lyapunov exponents from time series," Int. J. Bifurcation Chaos **2**, 155–165 (1992).

[66]R. K. Benninger and D. W. Piston, "Cellular communication and heterogeneity in pancreatic islet insulin secretion dynamics," Trends Endocrinol. Metab. **25**, 399–406 (2014).

[67]D. Pipeleers, R. Kiekens, Z. Ling, A. Wilikens, and F. Schuit, "Physiologic relevance of heterogeneity in the pancreatic beta-cell population," Diabetologia **37**, S57–S64 (1994).

[68]C. F. Van Schravendijk, R. Kiekens, and D. G. Pipeleers, "Pancreatic beta cell heterogeneity in glucose-induced insulin secretion," J. Biol. Chem. **267**, 21344–21348 (1992).

[69]R. Albert, "Scale-free networks in cell biology," J. Cell Sci. **118**, 4947–4957 (2005).

[70]H. Song, C. C. Chen, J. J. Sun, P. Y. Lai, and C. K. Chan, "Reconstruction of network structures from repeating spike patterns in simulated bursting dynamics," Phys. Rev. E **90**, 012703 (2014).

[71]S. E. Kahn, R. L. Hull, and K. M. Utzschneider, "Mechanisms linking obesity to insulin resistance and type 2 diabetes," Nature **444**, 840–846 (2006).

[72]J. Rahier, Y. Guiot, R. Goebbels, C. Sempoux, and J.-C. Henquin, "Pancreatic β-cell mass in European subjects with type 2 diabetes," Diabetes, Obes. Metab. **10**, 32–42 (2008).